AIP | Applied Physics Letters

Band alignment of SnS/Zn(O,S) heterojunctions in SnS thin film solar cells

Leizhi Sun, Richard Haight, Prasert Sinsermsuksakul, Sang Bok Kim, Helen H. Park, and Roy G. Gordon

Citation: Applied Physics Letters **103**, 181904 (2013); doi: 10.1063/1.4821433
View online: http://dx.doi.org/10.1063/1.4821433
View Table of Contents: http://scitation.aip.org/content/aip/journal/apl/103/18?ver=pdfcov
Published by the AIP Publishing

Band alignment of SnS/Zn(O,S) heterojunctions in SnS thin film solar cells

Leizhi Sun,[1] Richard Haight,[2] Prasert Sinsermsuksakul,[3] Sang Bok Kim,[3] Helen H. Park,[1] and Roy G. Gordon[1,3,a)]
[1]School of Engineering and Applied Sciences, Harvard University, Cambridge, Massachusetts 02138, USA
[2]IBM T.J. Watson Research Center, Yorktown Heights, New York 10598, USA
[3]Department of Chemistry and Chemical Biology, Harvard University, Cambridge, Massachusetts 02138, USA

(Received 23 May 2013; accepted 22 August 2013; published online 29 October 2013)

Band alignment is critical to the performance of heterojunction thin film solar cells. In this letter, we report band alignment studies of SnS/Zn(O,S) heterojunctions with various compositions of Zn(O,S). Valence band offsets (VBOs) are measured by femtosecond laser pump/probe ultraviolet photoelectron spectroscopy (fs-UPS) from which conduction band offsets (CBOs) are calculated by combining with band gaps obtained by optical transmission/reflection measurements. The SnS/Zn(O,S) heterojunctions with S/Zn ratios of 0.37 and 0.50 have desirable small positive CBOs, while a ratio of 0.64 produces an undesirable large positive CBO. The results are consistent with the device performance of SnS/Zn(O,S) solar cells. © *2013 AIP Publishing LLC*.
[http://dx.doi.org/10.1063/1.4821433]

Tin (II) sulfide (SnS) has been widely recognized as a promising candidate to replace current thin film light-absorbing materials in photovoltaics. In addition to its non-toxic and earth-abundant nature, SnS shows several attractive properties, including suitable direct and indirect band gaps ($E_{g\ direct} \sim 1.3$–1.5 eV, $E_{g\ indirect} \sim 1.0$–1.1 eV), a large absorption coefficient ($\alpha > 10^4\,cm^{-1}$), intrinsic carrier concentration ($[p] \sim 10^{15}\,cm^{-3}$), and reasonably high mobility ($\mu \sim 10\ cm^2\ V^{-1}s^{-1}$).[1] There have been numerous reports on SnS-based thin film solar cells with various buffer layers, including SnS_2,[2] CdO,[3] Cd_2SnO_4,[3] CdS,[4–10] $Cd_{1-x}Zn_xS$,[7] ZnO,[11,12] TiO_2,[13] PbS,[14] and *a*-Si.[15] The prevalent low efficiencies can be attributed to various sources, such as bulk material impurities and defects, interface trap states, and notably unfavorable heterojunction band alignment.[16] Theory suggests that a small positive conduction band offset (CBO) in the range of 0 eV to +0.4 eV is the optimal band alignment.[17,18] Outside this range, a negative CBO suffers from increasing interface recombination, while a large positive CBO forms a barrier that reduces photocurrent collection. Although numerous SnS solar cells with different buffer layers have been fabricated, band alignment studies have only been reported for CdS,[16,19] SnO_2,[16] and ZnMgO.[20]

Zinc oxysulfide (Zn(O,S)) is an excellent candidate for a wide band gap buffer layer because its constituent elements can be tuned to give any composition ranging between ZnO and ZnS, hence forming a favorable CBO with various absorber layers.[21–25] The authors have reported SnS/Zn(O,S) thin film solar cells with a record high total area conversion efficiency of 2.04% certified by the National Renewable Energy Laboratory (NREL).[26] Devices with various compositions of Zn(O,S) were fabricated and characterized under illumination (~10 mW/cm^2) from a microscope halogen lamp (color temperature = 3300 K) as shown in Figure 1.[26] This illumination condition is sufficient to test for junction characteristics despite being different from the AM1.5 solar spectrum. The variation in Zn(O,S) composition was achieved by varying the ZnO:ZnS cycle ratio during the atomic layer deposition (ALD) process.[26] The three compositions of Zn(O,S) shown in Figure 1 have S/Zn ratios of 0.37, 0.50, and 0.58, corresponding to ZnO:ZnS cycle ratios of 7:1, 6:1, and 5.5:1, respectively. The current density-voltage characteristics suggest that the SnS/Zn(O,S) heterojunctions with S/Zn ratios of 0.37 and 0.50 have optimal CBOs, while the heterojunction with a higher ratio of 0.58 does not. It is believed that Zn(O,S) with a high S/Zn ratio forms an undesirable large positive CBO with SnS as the conduction band edge is known to rise with higher sulfur concentration.[27] In order to confirm the dependence of device performance on CBOs, precise measurements of band alignment of SnS/Zn(O,S) heterojunctions are needed.

Bare SnS and SnS/Zn(O,S) heterostructures were prepared for the band offset measurements. Soda-lime glass substrates were cleaned in solvents by sonication and then soaked in an oxidizing solution of NoChromix™ and sulfuric acid as an alternative to a chromic acid bath. Mo (200 nm) films were evaporated onto the substrates with an e-beam evaporator. SnS (500 nm) films were deposited onto the Mo-coated glass substrates at 200 °C by ALD through the reaction of a tin precursor, bis(*N*,*N*′-diisopropylacetamidinato)tin (II) ($Sn(MeC(N\text{-}iPr)_2)_2$), and hydrogen sulfide (H_2S).[1] Tin precursor vapor assisted by N_2 and a gas mixture of 4% H_2S in N_2 were injected sequentially into the deposition chamber to allow chemical reactions to occur successively on the substrate surface. In order to form SnS/Zn(O,S) heterojunctions, thin Zn(O,S) films (5 nm) of three different ZnO:ZnS cycle ratios (7:1, 6:1, and 5:1) were each deposited on top of SnS (500 nm) at 120 °C through the reaction of diethylzinc ($Zn(C_2H_5)_2$) with deionized water (H_2O) and hydrogen sulfide (H_2S), respectively. Based on Rutherford backscattering spectroscopy (RBS) analysis, the three cycle ratios were found to correspond to S/Zn ratios of 0.37, 0.50, and 0.64, respectively. To ensure the quality of the heterojunction interface, Zn(O,S) was deposited on top of the SnS without breaking vacuum. After film growth, the samples were sealed in a nitrogen-filled container to minimize surface oxidation during

a)Electronic mail: gordon@chemistry.harvard.edu

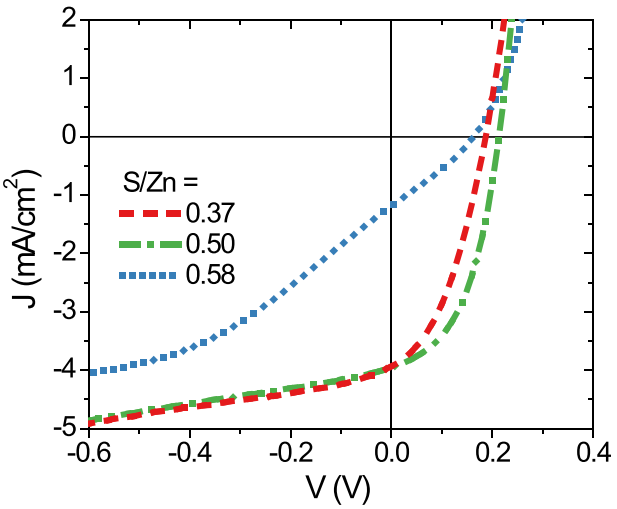

FIG. 1. Current density-voltage characteristics of Mo/SnS/Zn(O,S)/ZnO/ITO thin film solar cells with various compositions of Zn(O,S) under microscope lamp illumination (~10 mW/cm^2). Reprinted with permission from Appl. Phys. Lett. **102**, 053901 (2013). Copyright 2013 American Institute of Physics.

sample transfer. Transfer to the ultra-high vacuum UPS analysis system exposed the samples to less than 5 min of room atmosphere. Any adsorbed atmospheric water was desorbed by annealing to 150 °C for 10 s while under vacuum.

The valence band offsets (VBOs) of the SnS/Zn(O,S) heterojunctions were measured by using femtosecond ultraviolet photoelectron spectroscopy (fs-UPS). Fs-UPS measures key heterojunction electronic properties, such as valence band maximum (VBM), band bending, and Fermi level under flat band conditions. This technique has recently been applied to a number of absorber/buffer heterostructures.[28–30] Briefly, fs-UPS utilizes synchronized 800 nm (1.55 eV) pulses of photons from an amplified Ti:sapphire laser system operating at a 1 kHz repetition rate. The light pulses are split into time-synchronized pump and probe arms. The probe pulses are frequency up-converted to energies ranging from 15 to 40 eV by high harmonic generation in Ar gas and are spectrally selected and focused onto the sample for measurements. Typically, 26.35 eV photons (17th harmonic) are used to generate fs-UPS spectra. To extract the band bending at the heterojunctions, the pump pulses are focused on the probe area. This generates an electron-hole population in SnS that screens the static dipole field in the depletion region and flattens the SnS bands, resulting in a rigid energetic shift of the spectrum. The band bending of the SnS is determined by measuring this shift. Since the 800 nm (1.55 eV) pump pulses cannot be absorbed in Zn(O,S), the Zn(O,S) bands are not flattened and the band bending cannot be measured. To circumvent this problem, the Zn(O,S) layer was kept thin so that any small band bending in this layer would only minimally impact the band offsets extracted from the measurements.

Figure 2(a) shows the fs-UPS spectra for unpumped and pumped bare SnS. The VBM of SnS under flat band conditions was identified from the pumped spectrum by linear extrapolation of the valence band edge to zero intensity. The extrapolation yielded a binding energy of 0.28 eV relative to the Fermi level in the bulk. As shown in Figure 2(a), there is a 0.08 eV shift to a lower binding energy of the pumped spectrum relative to the unpumped one, confirming the p-type nature of SnS. The acceptor level energy due to tin vacancies is in close proximity to the Fermi level according to temperature-dependent Hall measurements. Figure 3 shows the temperature dependence of the majority carrier density of SnS from which the activation energy of tin vacancies was estimated to be 0.25 eV,[31] close to the measured Fermi level of 0.28 eV. From a theoretical point of view, the calculated tin vacancy formation enthalpy requires the acceptor level energy to be below 0.5 eV,[32] which is satisfied by the fitted value of 0.25 eV.

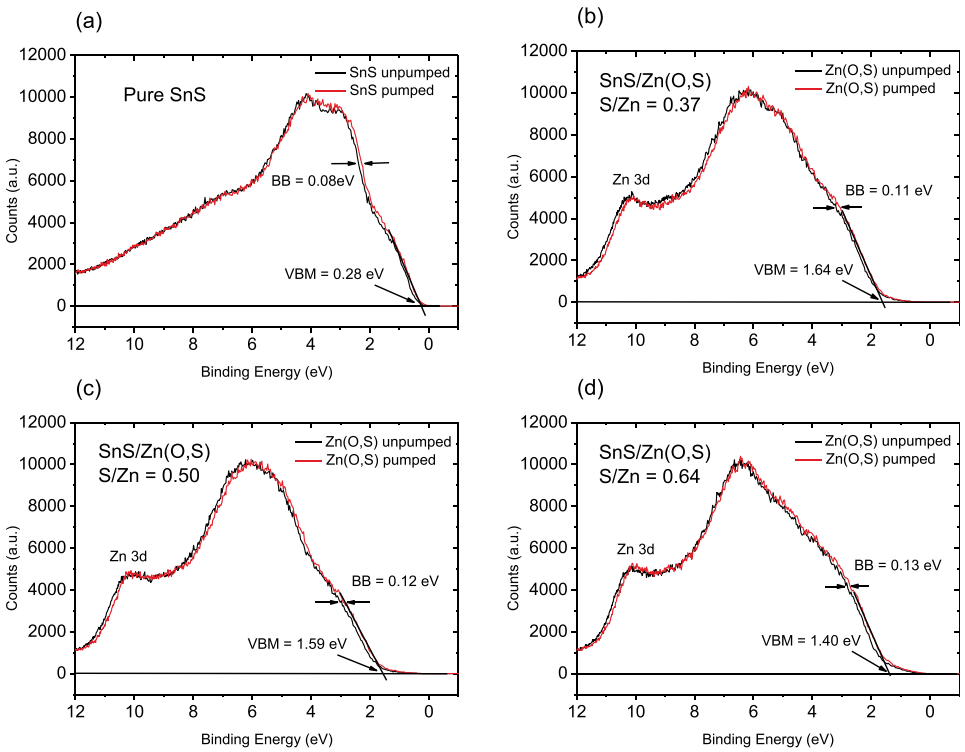

FIG. 2. Comparison of unpumped and pumped fs-UPS spectra for (a) bare SnS and SnS/Zn(O,S) heterostructures with S/Zn ratios of (b) 0.37, (c) 0.50, and (d) 0.64, from which the Fermi level, VBOs, and band bending are identified.

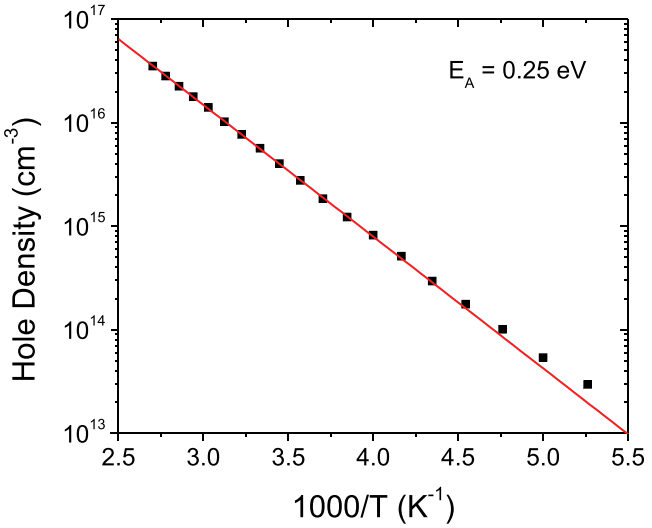

FIG. 3. Temperature dependence of majority carrier density for SnS from which the activation energy of tin vacancies is estimated to be 0.25 eV.

Figures 2(b)–2(d) display the fs-UPS spectra for unpumped and pumped SnS/Zn(O,S) heterostructures with increasing S/Zn ratios of 0.37, 0.50, and 0.64, respectively. For each S/Zn ratio, the VBM of pumped (flat band) SnS/Zn(O,S) was identified and the band bending in the underlying SnS layer was extracted. The VBO between SnS and Zn(O,S) was obtained by comparing the VBM of bare SnS and SnS/Zn(O,S) under flat band conditions. The SnS band bending and VBOs for the three compositions of Zn(O,S) are listed in Table I. The band bending of SnS is similar for the three ratios and corresponds to the dipole field induced as the n-type Zn(O,S) transfers negative charges to the p-type SnS. With an increasing S/Zn ratio, the VBM of Zn(O,S) moves to a lower binding energy, causing the VBO to decrease, as illustrated in the electronic structure diagram in Figure 5.

Once the VBOs of the SnS/Zn(O,S) heterojunctions have been determined, the optical band gaps are needed to derive the CBOs. SnS (500 nm) and Zn(O,S) (100 nm) were each deposited on quartz substrates for optical characterizations. Transmittance (T) and reflectance (R) spectra of SnS and Zn(O,S) were measured by ultraviolet-visible-near-infrared (UV-vis-NIR) spectrophotometry (Hitachi U-4100 UV-vis-NIR spectrophotometer). Film thickness was determined by cross-section scanning electron microscopy (Carl Zeiss Ultra 55 FESEM). Absorption coefficients α were obtained by relation $\alpha \approx 1/d \ln((1-R)/T)$, where d is the film thickness. Due to its polycrystalline nature, SnS has a well-defined gap in the density of states distribution. Crystalline direct and indirect band gaps can be determined from the plots of $(\alpha h\nu)^2$ versus $h\nu$ and $(\alpha h\nu)^{1/2}$ versus $h\nu$ by linearly extrapolating to $(\alpha h\nu)^2 = 0$, respectively.[1] SnS was found to have a direct band gap of 1.28 eV and an indirect band gap of 1.10 eV, both of which are consistent with reported values.[1,33–41]

The optical band gaps of Zn(O,S) are more difficult to determine. The optical properties of Zn(O,S) prepared by various methods have been extensively studied.[21,22,24,25,27,42–46] Since there is a 16% lattice mismatch between hexagonal ZnO and cubic or hexagonal ZnS, Zn(O,S) with intermediate compositions experience decreased crystallinity and become either nanocrystalline or amorphous, or a mixture of both, in the range of $0.3 < S/Zn < 0.6$.[21,22,27,42,43] Zn(O,S) with S/Zn ratios of 0.37, 0.50, and 0.64 essentially fall into this intermediate range. Based on X-ray diffraction (XRD) analysis (not shown here), the three compositions are either highly disordered nanocrystalline or amorphous as they do not exhibit significant diffraction features. Other XRD analyses also confirm this finding.[22,27] The decrease in crystallinity in the intermediate range results in band gap bowing with a band gap minimum around halfway between ZnO and ZnS, where the lattice strain causes the films to separate into a two-phase structure.[24,43,44] Because of the decreased crystallinity, the intermediate compositions exhibit long low energy absorption tails that make band gap extraction difficult.[22] The tailing effect of Zn(O,S) with S/Zn ratios of 0.37, 0.50, and 0.64 can be observed in the fs-UPS spectra in Figure 2. Unlike polycrystalline SnS with a well-defined band gap, the three compositions of Zn(O,S) show significantly larger tailing of states into the band gap. This tailing effect introduces an uncertainty in determining the band gaps of Zn(O,S) and the CBOs of the heterojunctions.

For direct band-to-band transitions in crystalline films, band gaps are determined by linearly extrapolating the plot of $(\alpha h\nu)^2$ versus $h\nu$ to zero, while for amorphous films, band gaps are identified from the plot of $(\alpha h\nu)^{1/2}$ versus $h\nu$ based on the Tauc model.[27,46–50] Since the three compositions of Zn(O,S) could be either nanocrystalline or amorphous, two sets of band gaps were extracted from the same absorption spectra to account for both scenarios, as illustrated in Figures 4(a) and 4(b). In Figure 4(a), the band gaps of Zn(O,S) with S/Zn ratios of 0.37, 0.50, and 0.64 were determined to be $E_g = 2.63$, 2.78, and 3.08 eV, respectively, if the films were treated as nanocrystalline. Meanwhile, in Figure 4(b), the band gaps of the same films were found to be $E_g = 2.57$, 2.68, and 2.92 eV, respectively, if the films were treated as amorphous. The tailing effect in the optical measurements introduces an uncertainty of 10% in determining the band gaps. The shift of the absorption edge shows a clear trend of a larger band gap with an increasing S/Zn ratio as shown in Figure 4. These band gaps are comparable with reported theoretical and experimental values.[22,24,25,27,43,44,46,51]

TABLE I. Electronic properties of SnS/Zn(O,S) heterostructures with S/Zn ratios of 0.37, 0.50, and 0.64.

S/Zn	VBO (eV)	SnS band bending (eV)	Zn(O,S) E_g (eV) (crystalline)	Zn(O,S) E_g (eV) (amorphous)	CBO (eV) (crystalline)	CBO (eV) (amorphous)
0.37	1.36 ± 0.05	0.11 ± 0.02	2.63 ± 0.25	2.57 ± 0.25	0.17 ± 0.25	0.11 ± 0.25
0.50	1.31 ± 0.05	0.12 ± 0.02	2.78 ± 0.25	2.68 ± 0.25	0.37 ± 0.25	0.27 ± 0.25
0.64	1.12 ± 0.05	0.13 ± 0.02	3.08 ± 0.25	2.92 ± 0.25	0.86 ± 0.25	0.70 ± 0.25

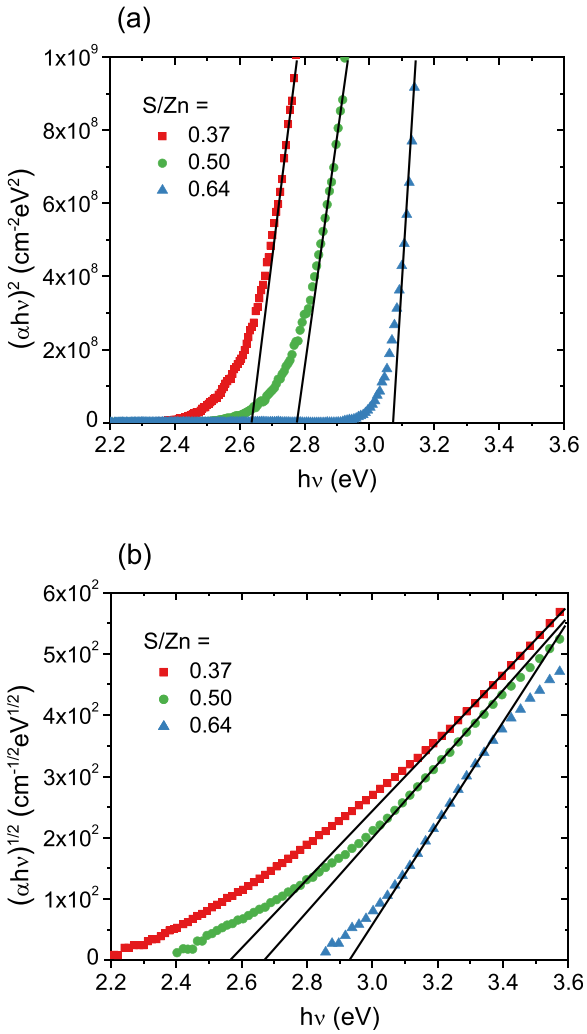

FIG. 4. Determination of the optical band gaps of various compositions of Zn(O,S) by treating the films as (a) nanocrystalline and (b) amorphous. (a) Plot of $(\alpha h\nu)^2$ versus $h\nu$ yields $E_g = 2.63$, 2.78, and 3.08 for Zn(O,S) with S/Zn ratios of 0.37, 0.50, and 0.64, respectively. (b) Plot of $(\alpha h\nu)^{1/2}$ versus $h\nu$ gives $E_g = 2.57$, 2.68, and 2.92 for Zn(O,S) with S/Zn ratios of 0.37, 0.50, and 0.64, respectively.

The CBOs of the SnS/Zn(O,S) heterojunctions were calculated by combining the VBOs measured by fs-UPS with the band gaps of SnS and Zn(O,S) derived from the absorption spectra (Table I). The electronic structure diagram of the SnS/Zn(O,S) heterostructures was constructed schematically in Figure 5. Since there are two sets of band gaps associated with Zn(O,S), the CBOs for the nanocrystalline scenario are shown next to the amorphous one (in parentheses) in Figure 5. As the S/Zn ratio increases from 0.37 to 0.64, the CBO increases as a result of both a decreasing VBO and an increasing band gap. For the SnS/Zn(O,S) heterojunctions with S/Zn ratios of 0.37 and 0.50, barriers of 0.17 eV (0.11 eV) and 0.37 eV (0.27 eV) are both sufficiently low to enable unimpeded minority current flow from the SnS absorber layer into the Zn(O,S) buffer layer, consistent with the high J_{sc} and large fill factor observed in Figure 1. For the SnS/Zn(O,S) heterojunction with a S/Zn ratio of 0.64, which is compared with the highest S/Zn-ratio device (S/Zn = 0.58) in Figure 1, the large barrier of 0.86 eV (0.70 eV) suppresses photocurrent collection, consistent with the observed lower J_{sc}, V_{oc}, and fill factor. While the band gaps of Zn(O,S) for the nanocrystalline and amorphous scenarios reveal relatively small quantitative differences that translate to equivalent differences in the CBOs, the same robust qualitative conclusions regarding minority carrier flow can be made. Hence, it is confirmed that CBOs play a critical role in the device performance of SnS/Zn(O,S) solar cells.

In summary, band alignment studies of SnS/Zn(O,S) heterojunctions with various compositions of Zn(O,S) were reported. The heterojunction VBOs, band bending, and Fermi level positions were extracted by fs-UPS. The band gaps were determined by optical transmission and reflection measurements. By combining these results, the CBOs were calculated and the electronic structure diagram was constructed. It was found that the SnS/Zn(O,S) heterojunctions with S/Zn ratios of 0.37 and 0.50 have desirable small positive CBOs, while the heterojunction with a S/Zn ratio of 0.64 produces an undesirable large positive CBO. The results,

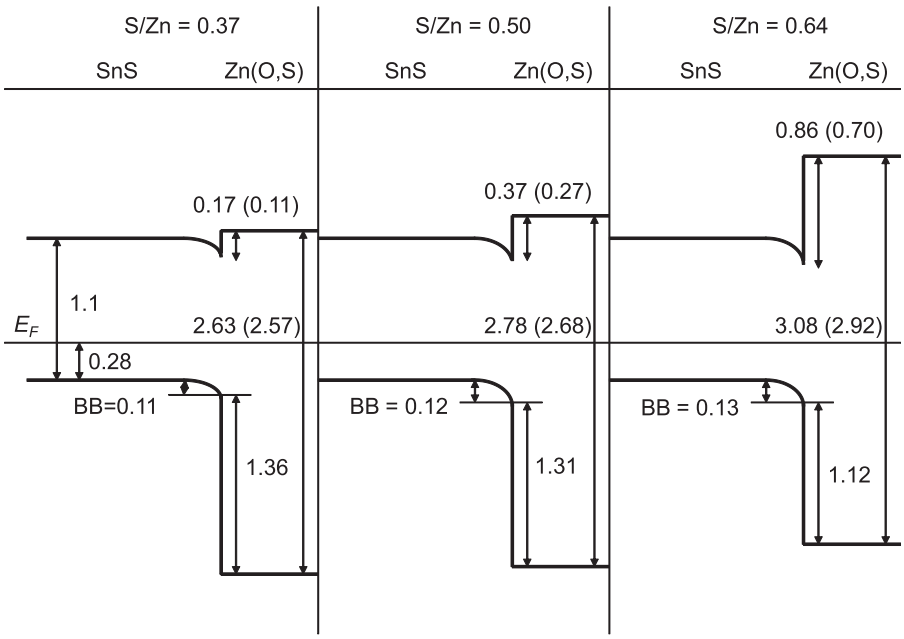

FIG. 5. Electronic structure diagram of Sn/Zn(O,S) heterostructures with S/Zn = 0.37, 0.50, and 0.64. The SnS band bending and VBOs are measured by fs-UPS, and the band gaps are determined from optical measurements. The CBOs for the nanocrystalline Zn(O,S) scenario are compared with the ones for the amorphous scenario as shown in parentheses. Despite quantitative differences, the same qualitative conclusions can be made.

consistent with previously measured solar cell characteristics, confirmed the critical dependence of device performance on CBOs. The measurement technique has been demonstrated as an effective tool for engineering band alignment in heterojunction thin film solar cells.

This work was supported by U.S. Department of Energy Contract No. DE-EE0005329 and by the U.S. National Science Foundation Award No. CBET-1032955. The experiments were conducted in part at Harvard University's Center for Nanoscale Systems (CNS), a member of the National Nanotechnology Infrastructure Network (NNIN), which was supported by the U.S. National Science Foundation under NSF Award No. ECS-0335765.

[1]P. Sinsermsuksakul, J. Heo, W. Noh, A. S. Hock, and R. G. Gordon, Adv. Energy Mater. **1**(6), 1116 (2011).
[2]A. Sanchez-Juarez, A. Tiburcio-Silver, and A. Ortiz, Thin Solid Films **480**, 452 (2005) .
[3]M. Ristov, G. Sinadinovski, M. Mitreski, and M. Ristova, Sol. Energy Mater. Sol. Cells **69**(1), 17 (2001).
[4]H. Noguchi, A. Setiyadi, H. Tanamura, T. Nagatomo, and O. Omoto, Sol. Energy Mater. Sol. Cells **35**(1–4), 325 (1994).
[5]K. T. R. Reddy, N. K. Reddy, and R. W. Miles, Sol. Energy Mater. Sol. Cells **90**(18–19), 3041 (2006).
[6]D. Avellaneda, G. Delgado, M. T. S. Nair, and P. K. Nair, Thin Solid Films **515**(15), 5771 (2007).
[7]M. Gunasekaran and M. Ichimura, Sol. Energy Mater. Sol. Cells **91**(9), 774 (2007).
[8]B. Ghosh, M. Das, R. Banerjee, and S. Das, Sol. Energy Mater. Sol. Cells **92**(9), 1099 (2008).
[9]O. E. Ogah, K. R. Reddy, G. Zoppi, I. Forbes, and R. W. Miles, Thin Solid Films **519**(21), 7425 (2011).
[10]S. A. Bashkirov, V. F. Gremenok, V. A. Ivanov, V. V. Lazenka, and K. Bente, Thin Solid Films **520**(17), 5807 (2012).
[11]M. Ichimura and H. Takagi, Jpn. J. Appl. Phys., Part 1 **47**(10), 7845 (2008).
[12]B. Ghosh, M. Das, P. Banerjee, and S. Das, Semicond. Sci. Technol. **24**(2), 025024 (2009).
[13]Y. Wang, H. Gong, B. H. Fan, and G. X. Hu, J. Phys. Chem. C **114**(7), 3256 (2010).
[14]A. Stavrinadis, J. M. Smith, C. A. Cattley, A. G. Cook, P. S. Grant, and A. A. R. Watt, Nanotechnology **21**(18), 185202 (2010).
[15]F. Jiang, H. L. Shen, W. Wang, and L. Zhang, J. Electrochem. Soc. **159**(3), H235 (2012).
[16]M. Sugiyama, K. T. R. Reddy, N. Revathi, Y. Shimamoto, and Y. Murata, Thin Solid Films **519**(21), 7429 (2011).
[17]A. Niemegeers, M. Burgelman, and A. Devos, Appl. Phys. Lett. **67**(6), 843 (1995).
[18]T. Minemoto, T. Matsui, H. Takakura, Y. Hamakawa, T. Negami, Y. Hashimoto, T. Uenoyama, and M. Kitagawa, Sol. Energy Mater. Sol. Cells **67**(1–4), 83 (2001).
[19]M. Ichimura, Sol. Energy Mater. Sol. Cells **93**(3), 375 (2009).
[20]K. T. R. Reddy, K. Ramya, G. Sreedevi, T. Shimizu, Y. Murata, and M. Sugiyama, Energy Procedia **10**, 172 (2011).
[21]E. B. Yousfi, T. Asikainen, V. Pietu, P. Cowache, M. Powalla, and D. Lincot, Thin Solid Films **361**, 183 (2000).
[22]C. Platzer-Bjorkman, T. Torndahl, D. Abou-Ras, J. Malmstrom, J. Kessler, and L. Stolt, J. Appl. Phys. **100**(4), 044506 (2006).
[23]A. Grimm, J. Just, D. Kieven, I. Lauermann, J. Palm, A. Neisser, T. Rissom, and R. Klenk, Phys. Status Solidi (RRL) **4**(5–6), 109 (2010).
[24]A. Grimm, D. Kieven, R. Klenk, I. Lauermann, A. Neisser, T. Niesen, and J. Palm, Thin Solid Films **520**(4), 1330 (2011).
[25]D. Kieven, A. Grimm, I. Lauermann, M. C. Lux-Steiner, J. Palm, T. Niesen, and R. Klenk, Phys. Status Solidi (RRL) **6**(7), 294 (2012).
[26]P. Sinsermsuksakul, K. Hartman, S. B. Kim, J. Heo, L. Z. Sun, H. H. Park, R. Chakraborty, T. Buonassisi, and R. G. Gordon, Appl. Phys. Lett. **102**(5), 053901 (2013).
[27]C. Persson, C. Platzer-Bjorkman, J. Malmstrom, T. Torndahl, and M. Edoff, Phys. Rev. Lett. **97**(14), 146403 (2006).
[28]D. Lim, R. Haight, M. Copel, and E. Cartier, Appl. Phys. Lett. **87**(7), 072902 (2005).
[29]R. Haight, A. Barkhouse, O. Gunawan, B. Shin, M. Copel, M. Hopstaken, and D. B. Mitzi, Appl. Phys. Lett. **98**(25), 253502 (2011).
[30]D. A. R. Barkhouse, R. Haight, N. Sakai, H. Hiroi, H. Sugimoto, and D. B. Mitzi, Appl. Phys. Lett. **100**(19), 193904 (2012).
[31]Y. S. Lee, M. T. Winkler, S. C. Siah, R. Brandt, and T. Buonassisi, Appl. Phys. Lett. **98**(19), 192115 (2011).
[32]J. Vidal, S. Lany, M. d'Avezac, A. Zunger, A. Zakutayev, J. Francis, and J. Tate, Appl. Phys. Lett. **100**(3), 032104 (2012).
[33]A. Tanusevski, Semicond. Sci. Technol. **18**(6), 501 (2003).
[34]N. K. Reddy and K. T. R. Reddy, Physica B **368**(1–4), 25 (2005).
[35]N. K. Reddy and K. T. R. Reddy, Mater. Res. Bull. **41**(2), 414 (2006).
[36]M. Devika, N. K. Reddy, K. Ramesh, K. R. Gunasekhar, E. S. R. Gopal, and K. T. R. Reddy, Semicond. Sci. Technol. **21**(8), 1125 (2006).
[37]M. Devika, K. T. R. Reddy, N. K. Reddy, K. Ramesh, R. Ganesan, E. S. R. Gopal, and K. R. Gunasekhar, J. Appl. Phys. **100**(2), 023518 (2006).
[38]M. Devika, N. K. Reddy, K. Ramesh, H. R. Sumana, K. R. Gunasekhar, E. S. R. Gopal, and K. T. R. Reddy, Semicond. Sci. Technol. **21**(10), 1495 (2006).
[39]E. Turan, M. Kul, A. S. Aybek, and M. Zor, J. Phys. D: Appl. Phys. **42**(24), 245408 (2009).
[40]F. Jiang, H. L. Shen, C. Gao, B. Liu, L. Lin, and Z. Shen, Appl. Surf. Sci. **257**(11), 4901 (2011).
[41]S. S. Hegde, A. G. Kunjomana, K. A. Chandrasekharan, K. Ramesh, and M. Prashantha, Physica B **406**(5), 1143 (2011).
[42]A. Takabayashi and S. Iida, Jpn. J. Appl. Phys., Part 2 **25**(6), L437 (1986).
[43]B. W. Sanders and A. Kitai, Chem. Mater. **4**(5), 1005 (1992).
[44]B. K. Meyer, A. Polity, B. Farangis, Y. He, D. Hasselkamp, T. Kramer, and C. Wang, Appl. Phys. Lett. **85**(21), 4929 (2004).
[45]S. Locmelis, C. Brunig, M. Binnewies, A. Borger, K. D. Becker, T. Homann, and T. Bredow, J. Mater. Sci. **42**(6), 1965 (2007).
[46]J. R. Bakke, J. T. Tanskanen, C. Hagglund, T. A. Pakkanen, and S. F. Bent, J. Vac. Sci. Technol. A **30**(1), 01A135 (2012).
[47]J. Tauc, R. Grigorov, and A. Vancu, Phys. Status Solidi B **15**(2), 627 (1966).
[48]J. Tauc, Mater. Res. Bull. **5**(8), 721 (1970).
[49]D. L. Wood and J. Tauc, Phys. Rev. B **5**(8), 3144 (1972).
[50]A. Ibrahim and S. K. J. Alani, Czech J. Phys. **44**(8), 785 (1994).
[51]C. Y. Moon, S. H. Wei, Y. Z. Zhu, and G. D. Chen, Phys. Rev. B **74**(23), 233202 (2006).